

The Use of Borneol as an Enhancer for Targeting Aprotinin-Conjugated PEG-PLGA Nanoparticles to the Brain

Lin Zhang · Limei Han · Jing Qin · Weiyue Lu · Jianxin Wang

Received: 28 August 2012 / Accepted: 4 April 2013 / Published online: 25 April 2013
© Springer Science+Business Media New York 2013

ABSTRACT

Purpose To evaluate the effect of borneol on the brain targeting efficiency of aprotinin-conjugated poly (ethyleneglycol)–poly (L-lactic-co-glycolic acid) nanoparticles (Apr-NP) and the activity of huperzine A (Hup A) loaded nanoparticles to AD rats .

Method Apr-NP was prepared by emulsion and solvent evaporation method. The uptake of Apr-NP alone or combined with borneol by brain capillary endothelial cells (BCECs) was evaluated by incorporating coumarin-6 as a tracer. *In vivo* imaging and the distribution of Hup A in the brain were measured to investigate the brain delivery of Apr-NP in rats, with or without the oral administration of borneol. Morris water maze was used to evaluate the memory improvement effect of Hup A loaded nanoparticles (Apr-NP-Hup).

Results Co-incubation with borneol could increase the uptake of nanoparticles by BCECs. Nanoparticles delivered into the rat brain were enhanced significantly by the co-administration of borneol. The pharmacological effects of Hup A loaded nanoparticles on improving the memory impairment of AD rats were greatly improved when combined with borneol.

Conclusions Borneol is a promising enhancer for brain-targeting delivery systems. When co-administered with aprotinin-modified nanoparticles, borneol could improve the brain targeting efficiency of nanoparticles significantly.

KEY WORDS aprotinin · borneol · brain targeting · huperzine A · nanoparticles

ABBREVIATIONS

AD	Alzheimer's disease
Apo E	Apolipoprotein E
APP	β-amyloid precursor protein
Apr	Aprotinin
Apr-NP	Aprotinin modified nanoparticles
Apr-NP-C6	Coumarin-6 labeled Aprotinin modified nanoparticles
Apr-NP-DiR	DiR labeled Aprotinin modified nanoparticles
Apr-NP-Hup A	Huperzine A loading Aprotinin modified nanoparticles
Apr-PEG-PLGA	Aprotinin modified poly (ethylene glycol- lactic-co-glycolic acid)
AUC	Area under curve
BBB	Blood–brain barrier
BCECs	Brain capillary endothelial cells
CNS	Central nervous system
DCM	Dichlormethane
DiR	1,1'-dioctadecyl-3,3,3'-tetramethyl indotricarbocyanine iodide
EE	Entrapping efficiency
HE	Hematoxylin and eosin
HPLC	High-performance liquid chromatography
Hup A	Huperzine A
Hup B	Huperzine B
Ig	Intragastric administration
IV	Intravenous administration
LRP	Low-density lipoprotein receptor-related protein

L. Zhang · L. Han · J. Qin · W. Lu · J. Wang (✉)
Department of Pharmaceutics, School of Pharmacy
Fudan University, 826 Zhangheng Rd.
Shanghai 201203, People's Republic of China
e-mail: jxwang@shmu.edu.cn

L. Zhang · L. Han · J. Qin · W. Lu · J. Wang
Key Laboratory of Smart Drug Delivery, Ministry of Education & PLA
Shanghai 201203, People's Republic of China

L. Zhang
Department of Pharmacy, Shaoxing People's Hospital, Shaoxing
Zhejiang 312000, People's Republic of China

Mal	Maleimide
Mal-PEG-PLGA	Maleimide-(ethylene glycol- lactic-co-glycolic acid)
MeOH	Methanol
mPEG-PLGA	Methoxy poly (ethylene glycol- lactic-co-glycolic acid)
N.S.	Normal saline
NP	Nanoparticles
NP -DiR	DiR labeled nanoparticles
NP -Hup A	Huperzine A loaded nanoparticles
NP-C6	Coumarin-6 labeled nanoparticle
PBS	Phosphate buffered saline
PEG	Polyethylene glycol
PLGA	Poly lactic-co-glycolic acid
RSD	Relative standard deviation
TEM	Transmission electron microscope

INTRODUCTION

Central nervous system (CNS) diseases are one of the largest and fastest-growing areas of unmet medical need. The major challenge to CNS drug delivery is the blood–brain barrier (BBB), which only permits highly lipid-soluble molecules under a threshold of 400–600 Daltons to penetrate (1,2). More than 98% of small-molecular-weight drugs and nearly 100% of large-molecular-weight drugs cannot cross the BBB. Finding ways to get therapeutic drugs to the CNS effectively, safely, and conveniently is an important task for researchers (3).

In the past decade, tremendous attention and effort focused on the development of modern and novel drug delivery systems to circumvent the BBB. Many effective approaches to transport drugs across the BBB, including using ligand-conjugation and nanotechnology to target the BBB *via* adsorptive or receptor-mediated transport of drug molecules, have been extensively studied (3–5). A successful strategy to increase drug penetration into the brain is to design nanoparticles that are transported into the brain using receptors that are naturally expressed at the BBB. This approach has been applied successfully with ligands to transferrin and insulin receptors (6–8). Low-density lipoprotein receptor-related protein (LRP) is a multi-ligand cell surface receptor that is highly expressed in vessel endothelial cells of BBB and has also been targeted for brain drug delivery recently. Its effect has been validated by the conjugation of drugs and nanocarriers with the ligands of LRP. Lipoproteins E (ApoE) and β -amyloid precursor protein (APP) were commonly used ligands because they possess Kunitz protease inhibitor (KPI) domain which can be recognized by LRP (9–12).

Aprotinin (Apr), obtained from bovine lung or pancreas, is a protease inhibitor with a molecular weight 6,512 Da. It also possesses a KPI domain and has high affinity with LRP. Studies have demonstrated that the transcytosis efficiency of Apr crossing bovine brain capillary endothelial cell (BBCEC) monolayers is at least 10-fold higher than that of transferrin. Study clearly showed that Apr crosses the BBB much more efficiently than other proteins (13) and suggested that Apr might be a promising targeting ligand in brain delivery systems.

Borneol, a simple bicyclic monoterpene, is widely used in traditional Chinese medicine as a messenger drug (14). It could enhance drug permeation through skin, gastrointestinal mucous membrane, nasal mucosa, cornea and the BBB. Recent studies have shown that borneol can accelerate the open of BBB and enhances the distribution of drugs in brain tissue (15,16). Cai *et al.* reported that compared with given alone, gastrodin co-administrated with borneol could be absorbed rapidly from the gastrointestinal tract. The peak time of gastrodin in the plasma became shorter (5–15 *vs* 30 min). The bioavailability of gastrodigenin, the main metabolite of gastrodin, in the brain was increased by 33.6–108.8% (17). Gao *et al.* found that the distribution of puerarin in brain tissues was significantly increased and its elimination was noticeably slower with borneol pretreatment (18). After oral administration of 15, 30, 90 mg·kg⁻¹ of borneol, oral bioavailability of tetramethylpyrazine phosphate in brain tissue was increased for 1.12, 1.62, 1.93 times respectively, compared to administration without borneol (19). Although borneol has been proved to be capable of promoting drugs into the brain efficiently, there have been few reports about the effect of borneol on the transport of nanocarriers through the BBB. It is interesting to know if borneol can increase the brain distribution of nanoparticles as well as pure compounds, which will provide a simple, non-toxicity and non-immunogenicity way for brain targeting.

The present study was undertaken to combine the modification with aprotinin and the brain enhancement of borneol of nanoparticles and evaluate the effect of borneol on the distribution of Apr-NPs to the brain *in vitro* and *in vivo*. Huperzine A (Hup A) was chosen as a model drug in this study. It is a lycopodium alkaloid isolated from the Chinese herb *Huperzia serrata* and has been approved to improve memory deficits in elderly people and AD patients in China (20,21). Hup A is a highly selective, reversible inhibitor of AChE and possesses a wide spectrum of neuroprotective activities, but its action is also inhibited by the low transport across the BBB (22).

In details, Apr was conjugated to poly (ethylene glycol)–poly (l-lactic-co-glycolic acid) nanoparticle (Apr-NP) as a novel biodegradable brain drug delivery system. The effect of borneol on the uptake capacity of Apr-NP-C6 was

validated using brain capillary endothelial cells (BCECs) *in vitro*. Then the brain delivery efficiency of intravenously administrated Apr-NP collaborated with intragastrically given of borneol PEG400 solution was investigated by *in vivo* optical imaging technique using DiR as a fluorescence probe on nude mice. Finally, the effect of Apr-NP-Hup A co-administrated with borneol on the improvement of memory impairment of AD was measured.

MATERIALS AND METHODS

Materials and Animals

Borneol was purchased from Huangpu Chemical Co. (Guangzhou, China); Aprotinin, DiR(1,1'-dioctadecyl-3,3,3',3'-tetramethyl indotricarbocyanine Iodide), coumarin-6 and A β 25–35 were purchased from Bio Basic(Toronto, CA), Biotium(Hayward, CA), Acros organics(Brussels BE) and Sigma-aldrich(St. Louis MO) respectively; Maleimide poly(ethylene glycol)-poly(lactic-co-glycolic acid) (Mal-PEG-PLGA) (MW 3.4 kDa–13 kDa) and methoxy poly(ethylene glycol)-poly(lactic-co-glycolic acid) (mPEG-PLGA) (MW 2.5 kDa–13 kDa) were obtained from the University of Electronical Science and Technology (Chengdu, China).

Mouse brain capillary endothelial cells (BCECs) were kindly provided by Prof. X. G. Jiang (School of pharmacy, Fudan University); Plastic cell culture dishes, plates and flasks were from Corning Incorporation (Lowell, USA); Fetal bovine serum (FBS) and Dulbecco's Modified Eagle Medium (high glucose) cell culture medium were purchased from Gibco (Carlsbad, USA); Double-distilled water was purified using a Millipore Simplicity System (Bedford, USA). All the other chemicals were of analytical grade and used without further purification.

The Balb/c nude mice (18~20 g, ♂) and Sprague-Dawley (SD) rats (200 g \pm 10 g, ♂) were obtained from the Experimental Animal Center of Fudan University and maintained at 22 \pm 2°C on a 12 h light-dark cycle with access to food and water *ad libitum*. The animals used for the experiment were treated according to the protocols evaluated and approved by the ethical committee of Fudan University.

Preparation and Characterization of NP and Apr-NP

Preparation of PEG-PLGA NP

Emulsion and solvent evaporation method was used to prepare the nanoparticles. In brief, 2 mg Mal-PEG-PLGA and 18 mg mPEG-PLGA were dissolved in 0.75 ml dichloromethane and 0.25 ml acetone. The solution was

then mixed with 2 ml 0.5% sodium cholate aqueous solution, emulsified using a probe sonicator to form o/w emulsion, which was further diluted into a 0.5% sodium cholate aqueous solution under magnetic stirring. Dichloromethane and acetone in the multiple emulsions were evaporated at a low pressure and 30°C using rotavapor. The formed nanoparticles were centrifuged at 21,000 g for 60 min and the precipitation was resuspended in 0.5 ml of 0.01 M HEPES buffer (pH 7.0) containing 0.15 M NaCl for further use (3).

Coumarin-6 loaded nanoparticles were prepared with the same procedure as above, Coumarin-6 were dissolved together with Mal-PEG-PLGA and mPEG-PLGA in dichloromethane and acetone and the obtained nanoparticles were subjected to a 1.5 \times 20 cm sepharose CL-4B column to remove untrapped coumarin-6. DiR or Hup A loaded nanoparticles were prepared with the same procedure as that for coumarin-6.

Preparation of Apr-NP

Apr was thiolated for 60 min with 30:1 molar ratio of 2-iminothiolane in 0.15 M pH 8.0 sodium borate buffer. The product was then applied to Hitrap™ Desalting column and eluted with 0.01 M pH 7.0 HEPES solutions. The protein fractions were collected and the introduced thiol groups were determined spectrophotometrically (λ =412 nm) with Ellman's reagent. Apr-NP were prepared by incubating the purified thiolated Apr with the NP at room temperature stirring for 8 h. The incubating medium is pH 7.0 HEPES and NaCl solutions and the molar ratio of Mal-PEG-PLGA in NP with the purified thiolated Apr is 1:2. The products were then subjected to a 1.5 \times 20 cm sepharose CL-4B column and eluted with 0.01 M pH 7.4 PBS to remove the unconjugated proteins (3).

Characterization of NP and Apr-NP

The mean diameter and zeta potential of the nanoparticles were determined by dynamic light scattering (DLS) method using a Zeta Potential/Particle Sizer (NICOMP™380 ZLS PSS, Santa Barbara, CA). The morphological examination of nanoparticles was carried out by transmission electron microscope (TEM) (H-600, Hitachi, Japan).

Measurement of Encapsulated Efficiency and Release Profile of Hup A-Loaded Nanoparticles

To measure the encapsulation efficiency (EE) of Hup A in different nanoparticles, drug-loaded nanoparticles were dissolved with acetonitrile and the concentration of Hup A was measured with HPLC (Agilent 1100, USA) (mobile phase: phosphate triethylamine methanol solution: water

50:50, $\lambda=306$ nm). EE was defined as the ratio between the Hup A amount detected by HPLC and theoretic feeding amount (23). The *in vitro* release profiles for Hup A of Apr modified or unmodified nanoparticles were performed at 37°C in 40 ml of 0.15 M PBS (pH 7.4) during 96 h and the concentration of Hup A in samples was analyzed by HPLC (24).

Cell Uptake of Apr-NP-C6 Enhanced by Borneol in BCECs Cells

BCECs were cultured in tissue culture dishes in Dulbecco's Modified Eagle Medium supplemented with 10% FBS, penicillin (100 U/ml) and streptomycin (100 mg/ml) (3). BCECs were seeded at a density of 10^4 cells/cm² onto 12-well plates and cultured for 24 h. After pre-incubated with HBSS for 15 min, the cells were incubated with Apr-NP-C6 or NP-C6 suspensions (15 µg/ml in HBSS, pH7.4) combined with borneol (0.1 mg/ml in HBSS, pH7.4) for 0.25 h at 37°C. At the end of the experiment, the cells were washed three times with HBSS (4°C) and observed under fluorescent microscope (Leica, DMI4000B, Germany) immediately. The cells were trypsinized for 2 min, collected, and tested of the fluorescence intensity using flow cytometry immediately for the quantitative measurement.

Effect of Borneol on the Distribution of Apr-NP Investigated by *In Vivo* Imaging Systems

The effect of the concentration of borneol on the distribution of NP in nude mice following vein injection was investigated by *In-Vivo* Imaging Systems (Kodak, Fx Pro/FX, USA). 12 nude mice (18–20 g) were separated to 4 groups randomly and anesthetized with 5% hydral (0.3 g/kg, i.p). NP-DiR was injected *via* intravenous route at the volume of 0.1 ml without borneol or with 0.1 ml of borneol PEG400 solution given intragastrically at 15, 30 or 60 mg/ml at the same time, respectively. The mice were anesthetized at pre-determined time and visualized in imaging systems. For imaging, the mice were placed in the light transparent chamber and the filters for excitation and emission were set at 730 nm and 790 nm respectively to measure fluorescence intensity of DiR (25).

The effect of borneol on the distribution of NP and Apr-NP in nude mice was investigated as the same procedure as above. Firstly, 12 nude mice (18–20 g) were divided into 4 groups randomly and anesthetized with 5% hydral (0.3 g/kg, i.p). Two groups were injected with 0.1 ml DiR-loaded NP or Apr-NP at the dose of 60 mg/kg. The other two groups were given DiR-loaded NP or Apr-NP and intragastrically administrated 0.1 ml of borneol PEG400 solution (30 mg/ml) at the same time. The fluorescence intensity of DiR in brain of each mouse was measured at 15 min, 30 min, 1 h, 2 h, 4 h, 8 h, 12 h, 24 h post administration, respectively.

In *ex vivo* imaging analysis test, nude mice were sacrificed by perfusion–fixation, and the brains were collected for fluorescence imaging at 30 min post administration.

Effect of Borneol on Brain Targeting of Apr-NP-Hup A in Mice

Animal Experiment

One hundred fifty mice (20 ± 2 g ♂) were randomly divided into 5 groups, 30 mice each group, fasted overnight before the experiment and free access to water. Different nanoparticles were injected from tail vein. The mice in group A, B and C were given Hup A solution (as control), NP-Hup A and Apr-NP-Hup A, respectively. For group D and group E, besides NP-Hup A and Apr-NP-Hup A, 0.1 ml borneol PEG400 solution (30 mg/ml) was administrated intragastrically at the same time. The dose calculated as Hup A is 1,000 µg/kg for each group. At the indicated time points (0.25, 1, 2, 4, 8 and 24 h) following drug administration, blood was collected into a heparinized centrifuge tube and centrifuged to obtain plasma. After the mice were sacrificed, the brains were immediately removed, washed with physiological saline, and dried with filter paper. The plasma and brain tissue samples were preserved in -20°C until analysis (26).

Samples Preparation

100 µl plasma was mixed with 20 µl Hup B solution (1 µg/ml, internal standard) and 2 mol/L NaOH solution to adjust pH to 11.8. The mixture was vortexed for 20 s, extracted with 1 ml ethyl acetate and centrifuged for 5 min at 10,000 rpm. The supernatant was dried with nitrogen. 50 µl mobile phase was added to the residue, vortexed for 30 s and centrifuged for 5 min (10,000 rpm). The supernatant was injected into the HPLC system for analysis.

Brain tissue sample was weighed and homogenized in physiological saline (1 g tissue/ml). Then the homogenate was mixed with 20 µl Hup B solution (1 µg/ml, internal standard) and 2 mol/L NaOH solution to adjust pH to 11.8. The following procedure was as the same as plasma sample.

Chromatographic Conditions

An HPLC method was developed to determine the concentration of Hup A in plasma and brain tissue. The analysis was performed on an Agilent 1100 series HPLC system (Agilent Technologies, USA) equipped with a quaternary pump, a vacuum degasser, a column thermostat, a UV detector and HP chemstation software. The separation was carried out using an Elite ODS column (250 mm×4.6 mm, 5 µm) protected by a Phenomenex guard column (4 mm×3 mm, ODS) under the following chromatographic conditions:

mobile phase A:B 50:50 (A: water-phosphoric acid triethylamine solutions (4 ml phosphate, 7 ml triethylamine plus 50% aqueous methanol (v/v) to 1,000 ml, the pH was adjusted to 3.2 with phosphoric acid); B: water), flow rate: 0.8 ml/min; column temperature: 25°C; detection wavelength: 308 nm; injection volume: 10 µl.

Data Analysis and the Calculation of Drug Targeting Index (DTI)

The pharmacokinetic parameters of Hup A in the plasma and the brain were calculated using Data and Statistics software package (DAS, Shanghai, China). The area under the curve (AUC) of Hup A in the brain and the plasma were calculated separately. The DTI was calculated to evaluate the brain targeting efficiency. The values of DTI are defined as (3):

$$DTI = \frac{(AUC_{\text{brain}}/AUC_{\text{plasma}})_{\text{Hup A-Apr-NP}}}{(AUC_{\text{brain}}/AUC_{\text{plasma}})_{\text{Hup A-NP}}}$$

Pharmacodynamic Study of Hup A Loaded Nanoparticles on AD Rats

Construction of AD Model of Rats

Adult male SD rats (200 g ± 10 g, ♂) were anesthetized with 10% hydral (0.5 g/kg, i.p.) and placed in a stereotaxic apparatus. Aβ25–35 peptide was dissolved in a sterile distilled physiological saline (5 mg/ml) and activated 4 days in 37°C. A hole was drilled into the skull (A 3.0 mm, L 2.2 mm, V 3.6 mm) of the rats and a microsyringe was placed into the hole with 3.6 mm deep under skull. 1 µl Aβ25–35 peptide solution was injected into the hippocampus within 10 min, held for 10 min and evacuated for 10 min. The same procedure was operated at the symmetric site of the hippocampus. Drugs were given 5 days after operation and the administration period was 10 days. Then the animals were used for Morris water maze test.

Morris Water Maze Test

A circular pool (180 cm diameter and 30 cm height) filled with water (22°C ± 1°C) was designed for Morris water maze (ANY-maze, stoelting USA) test. The pool was located in a dim, sound-proof test room with a visual cues, including a white-black colored poster on the wall, a lamp and a video on the top of the pool. Video tracking was conducted with a video camera focused on the full diameter of the pool (27).

Place navigation trail was used to train rats and record escape latency. The maze was divided into four quadrants. Four equally spaced points were served as starting positions

around the edge of the pool. A circular escape platform (12 cm diameter) was located in one quadrant, 1 cm below the water surface during the 20 times trails within 5 continuous days. For each trial, the rats were placed into the water maze at one of the four randomly determined locations. The heads of the rats were faced the center of the water maze. After the rat found and climbed onto the platform in 10 s, the trial was stopped, and the escape latency was recorded. If the rat did not climb onto the platform in 60 s, the trial was stopped too. Then the experimenter guided the rat to the platform and stayed for 10 s, and the escape latency was recorded as 60 s.

Space probe test was used to assess the spatial memory retention of the rats for the location of the hidden platform. During this trial, the platform was removed from the maze and the rats were allowed to search in the pool for 60 s. The pass times through the platform in quadrant 1 were recorded. All the parameters were analyzed by the video analysis system (ANY-maze).

Experiment Protocol

Sixty-three rats were randomly divided into nine groups ($n=7$). Group A is taken as normal control without any treatment. Group B is the sham operation group. 1 µl distilled sterile physiological saline water was injected into the hippocampus of the rats in the group. Group C was AD model group without any administration of drugs. Group D to Group F were AD models injected with Hup A, NP-Hup A and Apr-NP-Hup A solution, respectively. Group G and Group H were AD models treated with the injection of NP-Hup A or Apr-NP-Hup A combined with intragastric administration of 1 ml borneol PEG400 solution (30 mg/ml) at the same time, respectively; Group I was administrated intragastrically with 1 ml borneol PEG400 solution (30 mg/ml) only. The dose of Hup A in all groups was 0.5 mg/kg/d.

Data Analysis

All data were expressed as mean ± standard error of the mean (S.E.M). Statistical analysis was performed by one-way ANOVA followed by post hoc test of Student–Newman–Keuls for multi group comparison. Statistical significance was defined as $p < 0.05$.

RESULTS AND DISCUSSION

Characterization of NPs and Apr-NPs

Approaches using ligand-conjugation and nanotechnology *via* adsorptive or receptor-mediated transport have been

proved to be effective strategies to transport drugs across the BBB. In the present study, PEG-PLGA was chosen as drug carrier because of its biodegradability, high drug encapsulation efficiency and easy chemical modification *via* active terminal group of PEG. Aprotinin, which can be recognized by LRP, was conjugated to the nanoparticles to enhance the penetration through the BBB. The chemical diagram of the conjugation of aprotinin and PEG-PLGA was shown in Fig. 1. After conjugated with Apr, the particle size of nanoparticles was a little bigger than unconjugated ones, but still less than 100 nm.

The size of nanoparticles affects the endocytosis by the brain capillary cells. Nanoparticles under 100 nm that could be endocytosed by brain capillary endothelial cells were regarded as favorable for brain delivery (7). The nanoparticles prepared with emulsion and solvent evaporation method exhibited an average diameter under 100 nm before and after Apr conjugation. TEM photographs showed both the NP and Apr-NP were generally spherical and the particle size distributed in a narrow range (Fig. 2). Apr conjugation did not affect the size and the shape of nanoparticles. The nanoparticles prepared with the blend of mPEG-PLGA and MAL-PEG-PLGA exhibited an average diameter of 78 nm and increased to about 89 nm after Apr conjugation. The PDIs and zeta potentials of two kinds of nanoparticles before and after Apr conjugation were measured to be 0.048 ± 0.011 and 0.053 ± 0.013 , -24.2 ± 2.2 mV and -25.3 ± 3.8 mV, respectively. After encapsulation of Hup A, the average diameter, PDI, zeta potential and EE of NP were 85 nm, 0.049 ± 0.012 , -27.4 ± 2.9 mV and 86%, respectively. For Hup A loaded Apr-NP, the parameters were 91 nm, 0.052 ± 0.009 , -25.9 ± 2.7 mV

and 82% respectively. The results indicated that both NP and Apr modified NP were uniform, stable and with size less than 100 nm.

In vitro release study (Fig. 3) conducted in pH 7.4 PBS at 37°C showed that 50% and 56% of Hup A was released from NP and Apr-NP at 96 h, respectively, which indicated that sustained-release of Hup A could be achieved by the system. There was no significant difference between the release profiles of two groups, suggesting that Apr conjugation did not influence the release of Hup A from nanoparticles.

Effect of Borneol on the Uptake of NP-C6 and Apr-NP-C6 by BCECs

BCECs were recognized to represent the structural basis of BBB and have tight circumferential junctions between the cells. Therefore, BCECs were chosen to study the brain delivery of NP *in vitro* (3). As shown in Fig. 4I, the fluorescent intensity of Apr-NP in BCECs was higher than that of NP at 15 min post-incubation shown by fluorescence microscope. In Fig. 4II, flow cytometry quantitative results of the uptake of NP-C6 and Apr-NP-C6 within 1 h showed that there was an obviously increased amount of dye of Apr-NP in the cells compared with that of NP at 15, 30, 45 and 60 min, respectively. The uptake of NP and Apr-NP by BCECs was time-dependent within 1 h, which was believed related to the process of endocytosis. It could be found from Fig. 3 that the uptake of nanoparticles in combination with borneol was significantly improved, which indicated that both the modification of Apr and the co-incubation of borneol could increase the cell uptake of nanoparticles greatly.

Fig. 1 Chemical synthesis diagram of aprotinin and PEG-PLGA.

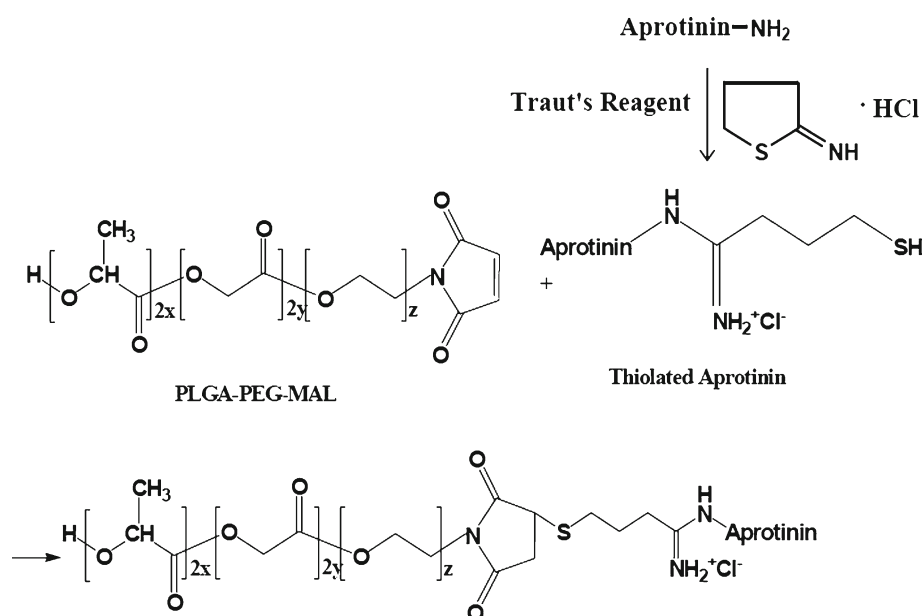
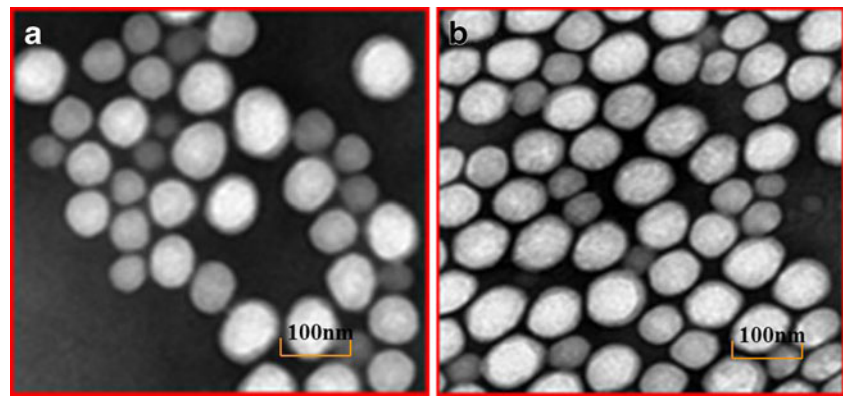


Fig. 2 Transmission electron micrographs of nanoparticles negatively stained with phosphotungstic acid. (a) NP; (b) Apr-NP.



The higher uptake of Apr-NP than NP in BCECs suggested that there was an active targeting mechanism involving LRP (13). It has been found that borneol can obviously loosen the intracellular tight junction in BBB and accelerate the transportation of substance through the intercellular passage, which might contribute to the enhanced uptake of NP and Apr-NP.

Effect of Borneol on the Distribution of NP and Apr-NP to the Brain

Effect of Different Concentration of Borneol on the Distribution of NP to the Brain

NP-DiR was injected into nude mice with intragastric co-administration of different concentration of borneol. *In vivo* fluorescent images were taken from 10 min to 24 h after administration. Figure 5I showed that the amount of DiR into the brain could be significantly increased by borneol. The improvement effect was concentration dependent but nonlinear related. The strong fluorescence in mouse brain at 10 min after administration indicated that borneol worked soon to enhance the permeation of NPs through the BBB. The concentration of 30 mg/ml and 60 mg/ml had a much stronger promotion of fluorescence than that of 15 mg/ml. No

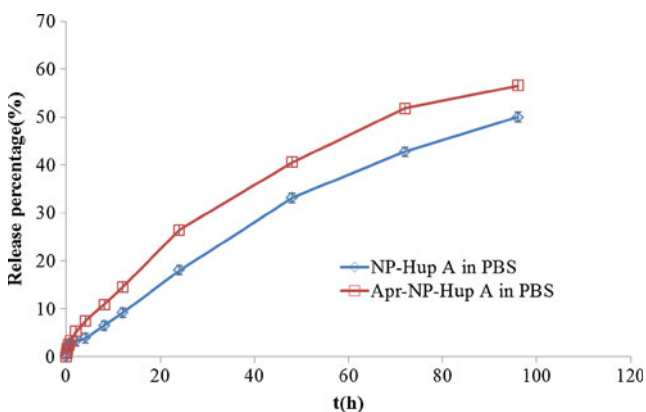


Fig. 3 Release profiles of Hup A from NP-Hup A and Apr-NP-Hup A ($n=3$).

obvious difference was observed between the group of 30 mg/ml and 60 mg/ml (Fig. 5II). The enhanced accumulation of DiR in brain with 30 mg/ml and 60 mg/ml of borneol could last more than 8 h. For 15 mg/ml borneol, however, the effect could be lasted less than 2 h. Based on the results, the dose of 30 mg/ml borneol was chosen in the following studies.

Effect of Borneol on the Distribution of NP and Apr-NP in the Brain

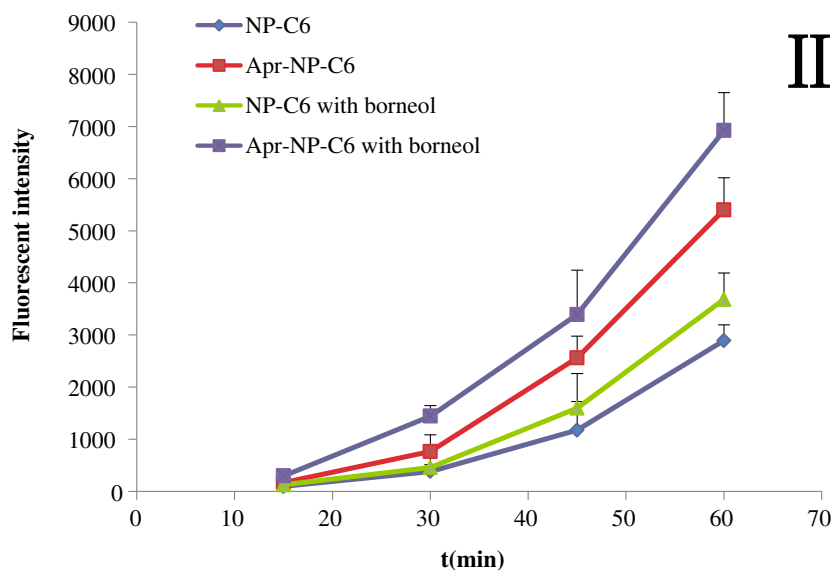
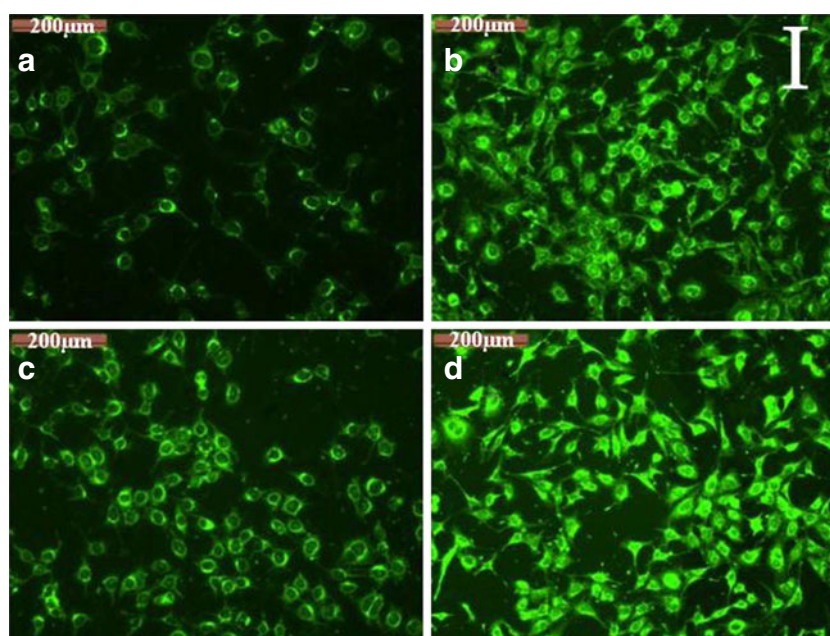
The results of qualitative and quantitative tests (Fig. 6) showed that the modification of Apr could increase the delivery of nanoparticles into the brain significantly within 8 h, compared with unmodified NP. When borneol was intragastrically co-administrated, the distribution of the nanoparticles into the brain could be enhanced further. It indicated that the distribution of nanoparticles in other organs was significantly increased at the same time, especially in the liver and the spleen. The result is similar to the previous report (28). Although the enhancing effect is closely related to the dose of borneol, ganciclovir solid lipid nanoparticles (GCVb-SLN3), which was modified with the highest amount of borneol, produced the highest AUC_{0-t} and C_{max} in the liver and spleen of all the tested formulations after injection into rats. With the modification of borneol, the C_{max} of all the SLNs showed statistically significance ($P<0.05$) compared with GCV (ganciclovir)-injection and GCV-SLN. The results mean that the SLNs modified with borneol have the advantage to delivery more of the formulated drugs to the organs. The reason for this may be that borneol could not only enhance drug permeation through BBB, but also other biological membranes, such as skin, gastrointestinal mucous membrane, nasal mucosa and cornea (17,29).

Effect of Borneol on Brain Targeting of Apr-NP-Hup A in Mice

Chromatography

The HPLC method established for the assay of Hup A in the plasma and the brain was specific and sensitive. There was no

Fig. 4 (I) Fluorescence microscope qualitative uptake of NP-C6 and Apr-NP-C6 joined with borneol (0.1 mg/ml) *in vitro* in 15 min. bar: 100 μ m. **(a)**: NP-C6, **(b)**: Apr-NP-C6, **(c)**: NP-C6 with borneol, **(d)**: Apr-NP-C6 with borneol. **(II)** Flowcytometry quantitative test of uptake of NP-C6 and Apr-NP-C6 with borneol *in vitro* within 1 h ($n=3$).



interference observed from endogenous components at the retention time of all the analytes in the chromatograms. The retention time of Hup B and Hup A was 5.12 and 6.65 min, respectively. The method for Hup A in the plasma and the brain both showed good linearity within the concentration range of 5–500 ng/ml. The limit of quantitation (LOQ) was estimated to be 5.0 ng/ml with an accuracy of 95.8% and RSD of 4.28%. The mean relative recovery was 101.3% and the RSDs of intra- and inter-day precision were less than 6.0%.

Pharmacokinetic Study

The concentration-time profiles of Hup A in the brain and the plasma within 24 h after injection of Hup A solution,

NP-Hup A and Apr NP-Hp A with or without co-administration of 30 mg/ml borneol are shown in Fig. 7. When injected as solution, the concentration of Hup A will decrease rapidly in the plasma. It could be found that when given as NP, the concentration of Hup A was greatly improved both in the brain and in the plasma. The modification of Apr and intragastric co-administration of borneol could increase the amount of Hup A in the brain. The effect of borneol was even higher than that of Apr. The combination of Apr modification of nanoparticles and intragastric co-administration borneol gave the highest distribution of Hup A in the brain, which showed there was a collaborative effect between them. However, both the intragastric administration of borneol and Apr modification of nanoparticles

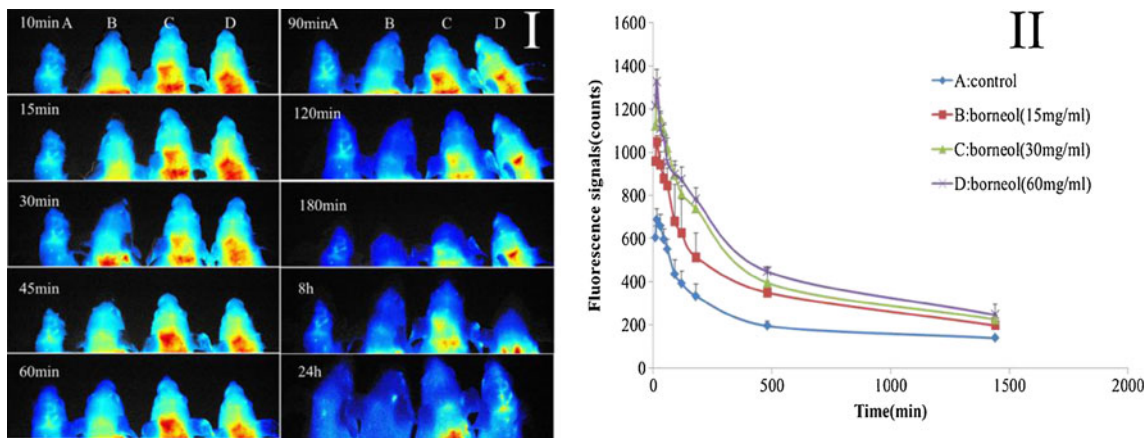


Fig. 5 (I) Qualitative imaging of the brains of nude mice administrated with NPs. A were the images of mice injected with NP without borneol as control. B, C and D were the images of mice injected with NPs and gastric perfusion of borneol at 15 mg/ml, 30 mg/ml and 60 mg/ml, respectively. (II) The fluorescence quantitative signals of nude mice administrated with NPs and gastric perfusion of borneol at 15 mg/ml, 30 mg/ml and 60 mg/ml, respectively within 24 h.

did not change the profile of NP-Hup A in the plasma obviously.

The DTI of every group was calculated according to the AUC of Hup A in the brain and the plasma to evaluate the brain targeting efficiency. The AUC and DTI values of Apr-NP-Hup A, NP-Hup A with borneol and Apr-NP-Hup A

with borneol, compared to NP-Hup A, were shown in Table I.

With the modification of Apr, the DTI of NP-Hup A was increased to 1.970, which showed that the conjugation of Apr could enhance the brain targeting of nanoparticles remarkably. When co-administrated with borneol, the DTIs of NP-

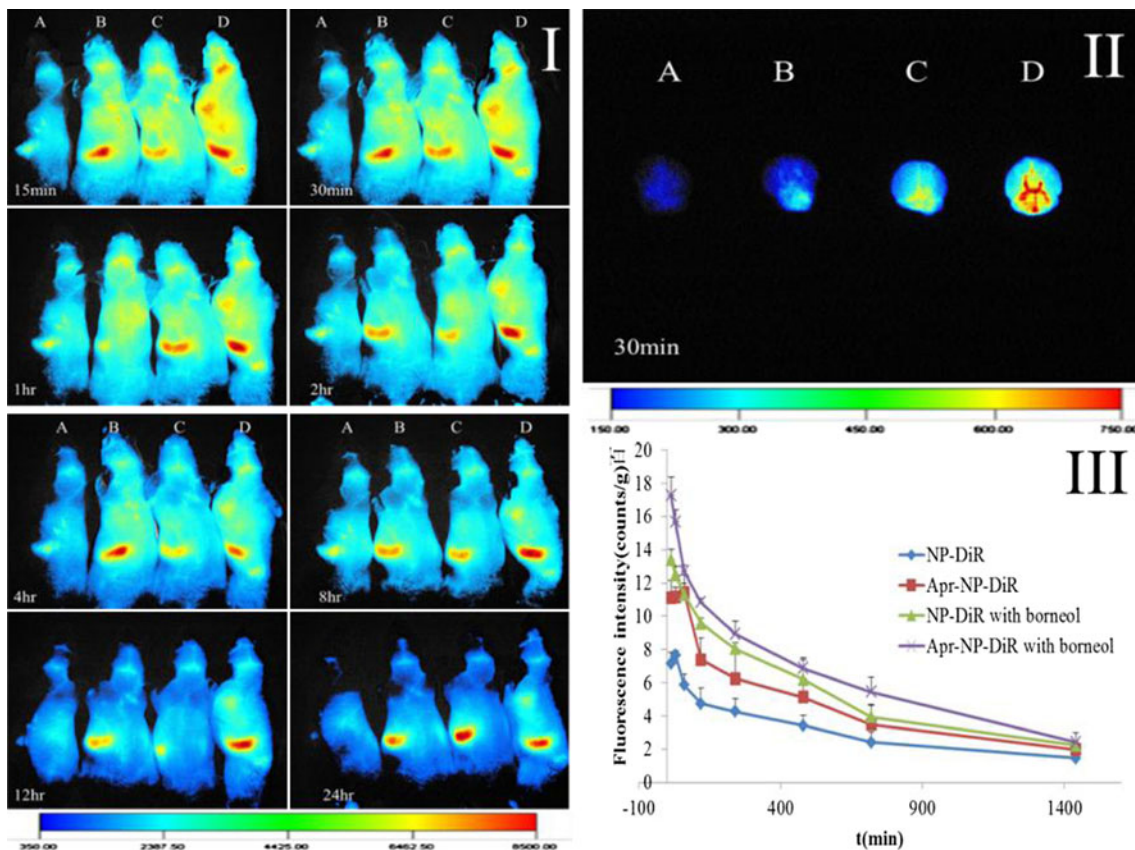


Fig. 6 Effect of borneol on the promotion of brain distribution of NP-DiR and Apr-NP-DiR in nude mice. (a): NP-DiR; (b): Apr-NP-DiR; (c): NP-DiR with borneol (d): Apr-NP-DiR with borneol (I) Qualitative test *in vivo* within 24 h; (II) Qualitative test *ex vivo* of mice brain after 30 min of administration. (III) Fluorescence intensity of DiR in mice brain within 24 h.

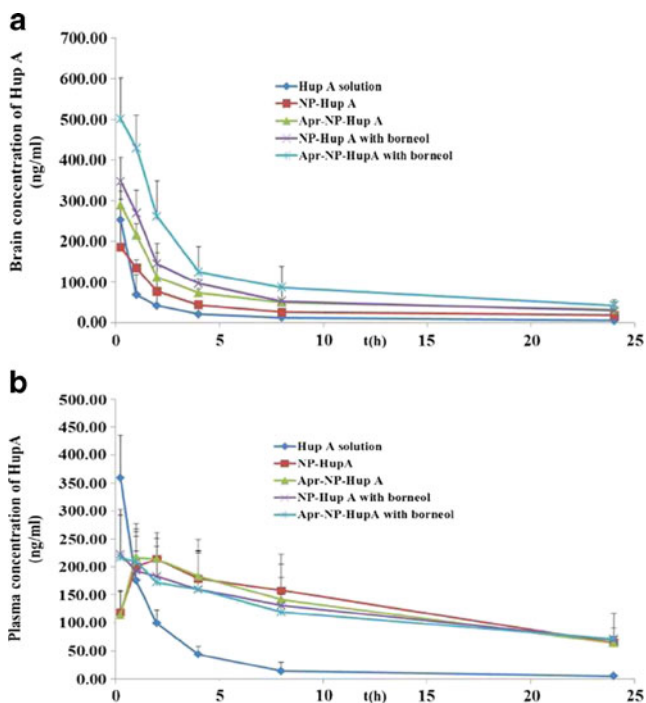


Fig. 7 The Hup A concentration-time profiles in the brain (a) and in the plasma (b) after iv Hup A solution, NP-Hup A and Apr-NP-Hup A with or without ig borneol in mice ($n = 5$).

Hup A and Apr-NP-Hup A were 1.863 and 2.712, respectively, both significantly improved. The results confirmed that the effect of borneol on the delivery of nanoparticles into the brain. When the modification of Apr and the enhancement of borneol applied simultaneously, the brain targeting efficiency of nanoparticles could be improved additionally.

Pharmacodynamic Study of Hup A Loaded Nanoparticles on AD Rats

Place navigation tests and space probe tests were performed using AD model rats to evaluate the pharmacodynamic effects of Hup A loaded nanoparticles on the improvement of memory impairment.

Place Navigation Test

The escape latency of the rats in Morris water maze test was recorded to evaluate the effect of Hup A loaded nanoparticles

on the recovery of injured memory of AD rats. The results of 20 trails during five continuous days were shown in Fig. 8.

It could be seen from Fig. 8 that during the 5 days, the escape latency of the normal rats was shortened gradually, indicating the memory of the rats on platform location could be gradually enhanced after training. Compared with group A, the memory improvement of the rats in group C was significantly slower ($p < 0.01$), which proved that the AD model induced by A β 25-35 was successful and could be used to verify the pharmacodynamics of Hup A preparations. No obvious difference of the escape latency of the rats between group B and group A was found, which meant that the trauma of the surgery itself did not induce memory impairment of the rats.

Although the memory recovery effect of Hup A solution was not so strong as group F, G and H, it could also improve the memory of AD rats which can be concluded from the significant difference between group D and group C ($p < 0.01$). However, the effect could not be lasted long because of the short half-life of Hup A. When encapsulated into nanoparticles and modified with Apr, Hup A could be delivered into the brain effectively and released sustainedly, which helped to achieve a longer and stronger effect.

There was no significant difference of the escape latency of the rats among groups in the first 2 days. From the third day, difference between groups began to appear and exhibited more obvious in the following 2 days. The difference ($p < 0.05$) between group E and F showed that Apr modification could enhance the transport of nanoparticles through BBB and release more Hup A in the brain to repair the memory damage in rats. Significant difference ($p < 0.05$) between group E and group G, group F and group H indicated that borneol could promote the delivery of NP-Hup A and Apr-NP-Hup A into the brain, thus improve memory impairment of AD rats. The enlarged significant difference between group E and group H ($p < 0.01$) confirmed that intragastric administration of borneol and Apr modification of nanoparticles have collaborate effect in delivering nanoparticles into the brain and improving memory impairment of AD rats.

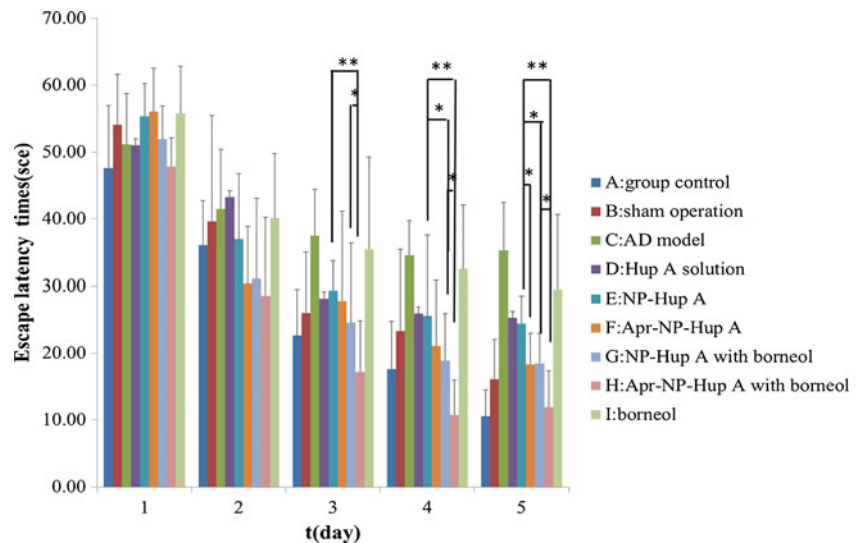
Space Probe Test

After 20 trails training in 5 days, spatial probe test of rats was conducted in the sixth day. As shown in Fig. 9, the test

Table 1 AUCs and DTIs of NP-Hup A and Apr-NP-Hup A alone or Combined with Borneol in Mice

	NP-Hup A	Apr-NP-Hup A	NP-Hup A with borneol	Apr-NP-Hup A with borneol
AUC in the brain (ng/ml•h)	1163	2118	2158	3189
AUC in plasma (ng/ml•h)	4604	4254	4584	4653
DTI	1	1.970	1.863	2.712

Fig. 8 Effect of NP-Hup A, Apr-NP-Hup A and with the combination of borneol on escape latency of rats in Morris water maze test in 20 trails during 5 days ($n = 7$).



results indicated that platform crossing times varied remarkably among groups.

The passing times of the rats in group C (AD model rats) were significantly less ($p < 0.01$) than that of group A (normal rats), indicating the AD rats model was successfully replicated in the study. There was no obvious difference of the times between group B and group A, which proved that the trauma of the surgery itself did not affect the memory of rats.

The results of the memory improvement effect of AD rats after the treatment with NP-Hup A and Apr-NP-Hup A alone, or combined with borneol, are consistent with those in place navigation test. In brief, both the Apr modification of the nanoparticles and the co-administration of borneol could increase the passing times significantly. When two strategies applied together, the effect could be mostly enhanced.

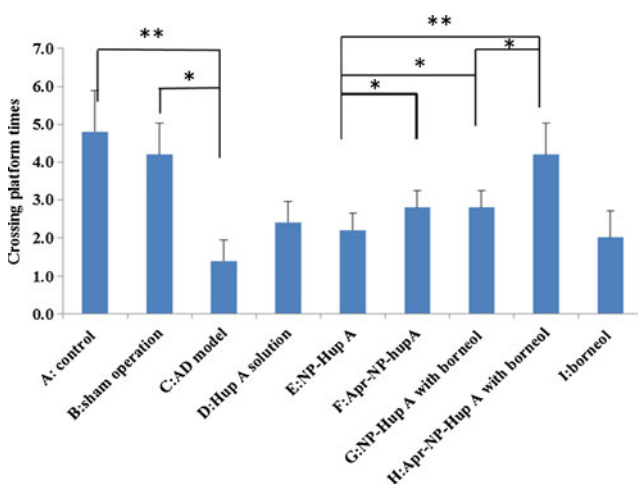


Fig. 9 The effect of Apr modification and co-administration of borneol on the passing times within 60s through the removed platform in space probe test ($n = 7$).

Amyloid β -peptide ($A\beta$) fragments has been implicated in neuronal and vascular degeneration, potentially contributing to progressive dementia in AD (30). Among the $A\beta$ fragments studied so far, $A\beta_{25-35}$ peptide represents the shortest fragment of $A\beta$ and exhibits significant levels of molecular aggregation, retaining the toxicity of the full length peptide. Therefore, $A\beta_{25-35}$ is frequently used in AD models. In present study, we successfully established AD model in rats induced by $A\beta_{25-35}$, which caused a significant disruption of learning and memory in hippocampus of rats (31).

Borneol is a small lipophilic compound and practically insoluble in water. It could be rapidly absorbed *via* gastrointestinal tract because of its liposolubility and low molecular weight (154.25). It was reported that the C_{max} of borneol in mice plasma was 3 min after intragastric administration. Therefore, borneol is commonly orally administrated. In this study, borneol solution was prepared using PEG 400 as solvent. Although loosening the intercellular tight junction of the BBB might be the main pathway of borneol to promote the passing of nanoparticles, the mechanisms involve multiple effects. It was reported that borneol could enhance epithelial junction permeability and then promote paracellular drug transportation after passing through the gastrointestinal mucous membrane (32). Chen and Wang reported that borneol could obviously loosen the intercellular tight junction in the BBB and accelerate the transportation of drugs through the intercellular passage (33), and significantly inhibit the activity of P-glycoprotein (34). It could also increase the number and volume of pinocytosis vesicles in BBB cells and then accelerate the transportation of drugs by cell pinocytosis (35). Li found that borneol could open the BBB by increasing levels of histamine and 5-hydroxy-tryptamine in hypothalamus (36). We also proved that borneol could promote the membrane fluidization of BCECs. It indicated that the combination of borneol and aprotinin had an additive effect on enhancing the

brain delivery of nanoparticles. It was not clear whether the two combined strategies mediate separate parallel proceeding transport mechanisms, transcytosis and paracellular transport, respectively, or synergize in a combined transport, either enhanced LRP-mediated transcytosis by borneol, or LRP receptor cell surface binding followed by paracellular transport on the outside of cells. It needs to be studied in our future work.

Borneol is a special promoter with a few pharmacological properties, such as acesodyne, sedation, anti-inflammation, antibiosis, etc. (37). It has been used as a brain refreshing drug in traditional Chinese medicine. It could be found from Figs. 8 and 9 that borneol alone could improve the memory impairment of the rats to some extent, although the effect was not significant and lasted only for a short time. Borneol was regarded as a messenger drug considered to be capable of introducing main effective drugs in the prescription to the target site to increase therapeutic efficacy. The results in our study confirmed the theory that “borneol has only weak effect if used alone, but if co-administrated with other drugs, it will improve the efficacy of the whole formulation” (37–39).

Until now, the mechanisms of borneol's effect on improving the brain delivery of nanoparticles are still not clearly clarified. Although the safety of borneol has been proved by numerous clinical applications, and it was reported borneol can increase the pathological opening of BBB and has a protective effect on brain tissue (40), the possible side effects of the use of borneol should not be ignored and need to be studied comprehensively. More studies on the mechanisms and safety of the application of borneol as a promoter for brain-targeting delivery are ongoing in our lab.

CONCLUSION

An aprotinin-mediated and borneol-promoted nanoparticles delivery system was developed and evaluated to improve brain drug targeting efficiency in the present study. It was demonstrated that both the modification of aprotinin and co-incubation with borneol could increase the uptake of nanoparticles by BCECs. Nanoparticles delivered into the brain were enhanced significantly by conjugation of aprotinin or co-administration of borneol. When the two strategies were applied together, the brain targeting efficiency could be elevated obviously further. The pharmacological effects of Hup A on improving the memory impairment of AD rats were greatly improved gradually by encapsulating into nanoparticles, modified with aprotinin, and combined with borneol. Thus, the results showed that borneol is not only a good enhancer to deliver compounds into brain, but also a promising promoter for brain-targeting nanocarriers.

ACKNOWLEDGMENTS AND DISCLOSURES

This work was supported by National Natural Sciences Fund of China (No.81001642) and National Basic Research Program of China (973 Program, 2007CB935800).

REFERENCES

- Abbott NJ, Patabendige AAK, Dolman DEM, Yusof SR, Begley DJ. Structure and function of the blood–brain barrier. *Neurobiol Dis.* 2010;37:13–25.
- Popescu BO, Toescu EC, Popescu LM, Bajenaru O, Muresanu DF, Schultzberg M, *et al.* Blood–brain barrier alterations in ageing and dementia. *J Neurol Sci.* 2009;283:99–106.
- Hu K, Li J, Shen Y, Lu W, Gao X, Zhang Q, *et al.* Lactoferrin-conjugated PEG-PLA nanoparticles with improved brain delivery: *in vitro* and *in vivo* evaluations. *J Control Release.* 2009;134:55–61.
- Huang R, Ke W, Han L, Liu Y, Shao K, Jiang C, *et al.* Lactoferrin-modified nanoparticles could mediate efficient gene delivery to the brain *in vivo*. *Brain Res Bull.* 2010;81:600–4.
- Lin LN, Liu Q, Song L, Liu FF, Sha JX. Recent advances in nanotechnology based drug delivery to the brain. *Cytotechnology.* 2010;62:377–80.
- Craparo EF, Bondi ML, Pitarresi G, Cavallaro G. Nanoparticulate systems for drug delivery and targeting to the central nervous system. *CNS Neurosci Ther.* 2011;17:670–7.
- Beduneau A, Saulnier P, Benoit JP. Active targeting of brain tumors using nanocarriers. *Biomaterials.* 2007;28:4947–67.
- Jonesand AR, Shusta EV. Blood–brain barrier transport of therapeutics *via* receptor-mediation. *Pharm Res.* 2007;24:1759–71.
- Demeule M, Currie J-C, Bertrand Y, Ché C, Nguyen T, Régina A, *et al.* Involvement of the low-density lipoprotein receptor-related protein in the transcytosis of the brain delivery vector Angiopep-2. *J Neurochem.* 2008;106:1534–44.
- Nazer B, Hong S, Selkoe DJ. LRP promotes endocytosis and degradation, but not transcytosis, of the amyloid- β peptide in a blood–brain barrier *in vitro* model. *Neurobiol Dis.* 2008;30:94–102.
- Bell RD, Sagare AP, Friedman AE, Bedi GS, Holtzman DM, Deane R, *et al.* Transport pathways for clearance of human Alzheimer's amyloid beta-peptide and apolipoproteins E and J in the mouse central nervous system. *J Cereb Blood Flow Metab.* 2007;27:909–18.
- Demeule M, Regina A, Che C, Poirier J, Nguyen T, Gabathuler R, *et al.* Identification and design of peptides as a new drug delivery system for the brain. *J Pharmacol Exp Ther.* 2008;324:1064–72.
- Demeule M, Currie JC, Bertrand Y, Che C, Nguyen T, Regina A, *et al.* Involvement of the low-density lipoprotein receptor-related protein in the transcytosis of the brain delivery vector angiopep-2. *J Neurochem.* 2008;106:1534–44.
- Bhatia S, Letizia C, Api A. Fragrance material review on borneol. *Food Chem Toxicol.* 2008;46:S77–80.
- Chai G, Pan Y, Li F. Effect of borneol/menthol eutectic mixture on nasal-brain delivery of neurotoxin loaded nanoparticles. *Zhongguo Zhong Yao Za Zhi.* 2009;34:698–701.
- Lu Y, Du SY, Chen XL, Wu Q, Song X, Xu B, *et al.* Enhancing effect of natural borneol on the absorption of geniposide in rat *via* intranasal administration. *J Zhejiang Univ Sci B.* 2011;12:143–8.
- Cai Z, Hou S, Li Y, Zhao B, Yang Z, Xu S, *et al.* Effect of borneol on the distribution of gastrodin to the brain in mice *via* oral administration. *J Drug Target.* 2008;16:178–84.

18. Gao CY, Li XR, Li YH, Wang LJ, Xue M. Pharmacokinetic interaction between puerarin and edaravone, and effect of borneol on the brain distribution kinetics of puerarin in rats. *J Pharm Pharmacol.* 2010;62:360–7.
19. Yanyu X, Qineng P, Zhipeng C. The enhancing effect of synthetical borneol on the absorption of tetramethylpyrazine phosphate in mouse. *Int J Pharm.* 2007;337:74–9.
20. Xiao XQ, Zhang HY, Tang XC. Huperzine A attenuates amyloid beta-peptide fragment 25-35-induced apoptosis in rat cortical neurons *via* inhibiting reactive oxygen species formation and caspase-3 activation. *J Neurosci Res.* 2002;67:30–6.
21. Wang R, Yan H, Tang XC. Progress in studies of huperzine A, a natural cholinesterase inhibitor from Chinese herbal medicine. *Acta Pharmacol Sin.* 2006;27:1–26.
22. Wang B-s, Wang H, Wei Z-h, Song Y-y, Zhang L, Chen H-z. Efficacy and safety of natural acetylcholinesterase inhibitor huperzine A in the treatment of Alzheimer's disease: an updated meta-analysis. *J Neural Transm.* 2009;116:457–65.
23. Zhan C, Gu B, Xie C, Li J, Liu Y, Lu W. Cyclic RGD conjugated poly(ethylene glycol)-co-poly(lactic acid) micelle enhances paclitaxel anti-glioblastoma effect. *J Control Release.* 2010;143:136–42.
24. Ye JC, Zeng S, Zheng GL, Chen GS. Pharmacokinetics of Huperzine A after transdermal and oral administration in beagle dogs. *Int J Pharm.* 2008;356:187–92.
25. Wen Z, Yan Z, Hu K, Pang Z, Cheng X, Guo L, et al. Odorranalectin-conjugated nanoparticles: preparation, brain delivery and pharmacodynamic study on Parkinson's disease following intranasal administration. *J Control Release.* 2011;151:131–8.
26. Chu D, Fu X, Liu W, Liu K, Li Y. Pharmacokinetics and *in vitro* and *in vivo* correlation of huperzine A loaded poly(lactic-co-glycolic acid) microspheres in dogs. *Int J Pharm.* 2006;325:116–23.
27. Mutlu O, Ulak G, Celikyurt IK, Akar FY, Erden F. Effects of olanzapine, sertindole and clozapine on learning and memory in the Morris water maze test in naive and MK-801-treated mice. *Pharmacol Biochem Behav.* 2011;98:398–404.
28. Ren J, Zou M, Gao P, Wang Y, Cheng G. Tissue distribution of borneol-modified ganciclovir-loaded solid lipid nanoparticles in mice after intravenous administration. *Eur J Pharm Biopharm.* 2013;83:141–148.
29. Wu CJ, Huang QW, Qi HY, Guo P, Hou SX. Promoting effect of borneol on the permeability of puerarin eye drops and timolol maleate eye drops through the cornea *in vitro*. *Pharmazie.* 2006;61:783–8.
30. Frozza RL, Horn AP, Hoppe JB, da Silva T, Simão F, Gerhardt D, et al. A β 1-42 and A β 25-35 peptides induce similar toxicity in organotypic hippocampal slice cultures and this effect can be prevented by resveratrol. *Alzheimers Dement.* 2009;5:P175.
31. Galoyan AA, Sarkissian JS, Chavushyan VA, Meliksetyan IB, Avagyan ZE, Poghosyan MV, et al. Neuroprotection by hypothalamic peptide proline-rich peptide-1 in A β 25-35 model of Alzheimer's disease. *Alzheimers Dement J Alzheimers Assoc.* 2008;4:332–44.
32. Zhou Y, Li W, Chen L, Ma S, Ping L, Yang Z. Enhancement of intestinal absorption of akebia saponin D by borneol and probenecid *in situ* and *in vitro*. *Environ Toxicol Pharmacol.* 2010;29:229–34.
33. Chenand YM, Wang NS. Effect of borneol on the intercellular tight junction and pinocytosis vesicles *in vitro* blood–brain barrier model. *Chin J Integr Tradit West Med.* 2004;24:632–4.
34. He H, Shen Q, Li J. Effects of borneol on the intestinal transport and absorption of two P-glycoprotein substrates in rats. *Arch Pharm Res.* 2011;34:1161–70.
35. Chenand YM, Wang NS. Effect of borneol on the intercellular tight junction and pinocytosis vesicles *in vitro* blood–brain barrier model. *Zhongguo Zhong Xi Yi Jie He Za Zhi.* 2004;24:632–4.
36. Li WR, Yao LM, Mi SQ, Wang NS. Relation of openness of blood–brain barrier with histamine and 5-hydroxy-tryptamine. *Chin J Clin Rehabil.* 2006;10:167–169.
37. Wei C, Wu G. Research advance in pharmacological effect of borneol and the underlying mechanism. *Int J Pathol Clin Med.* 2010;5:021.
38. Wu S, Cheng G, Feng Y. Progress in studies on pharmacology of borneol. *Chin Tradit Herb Drugs.* 2001;32:1143–4.
39. Wangand NS, Liang MR. Study of the effect of borneol on improving the activity of herbs. *J Tradit Chin Med.* 1994;35:46–7.
40. Zhao B, Liu Q. Comparison between borneol-induced opening of blood–brain barrier and its pathological opening. *Tradit Chin Drug Res Clin Pharmacol.* 2002;5:007.